Prostate Imaging – An Update

Bildgebung der Prostata – Ein Update

Authors T. Franiel[1], P. Asbach[2], U. Teichgräber[1], B. Hamm[2], S. Foller[3]

Affiliations
[1] Department of Diagnostic and Interventional Radiology, University Hospital Jena, Germany
[2] Department of Radiology, Campus Benjamin Franklin, University Medicine Berlin, Germany
[3] Department of Urology, University Hospital Jena, Germany

Key words
- prostate
- MR imaging
- ultrasound

received 23.2.2015
accepted 25.4.2015

Bibliography
DOI http://dx.doi.org/10.1055/s-0035-1553162
Published online: 26.6.2015
Fortschr Röntgenstr 2015; 187: 751–759 © Georg Thieme Verlag KG Stuttgart · New York · ISSN 1438-9029

Correspondence
Priv.-Doz. Dr. med. Tobias Franiel
Department of Diagnostic and Interventional Radiology, University Hospital Jena
Erlanger Alle 101
07747 Jena
Germany
Tel.: ++ 49/36 41/9 32 48 31
Fax: +49/36 41/9 32 48 32
tobias.franiel@med.uni-jena.de

Abstract

New technical and clinical developments of sonography and magnetic resonance imaging include improved detection, localization and staging as well as active surveillance of prostate cancer. Multiparametric MRI can best answer these typical clinical questions. However, ultrasound elastography seems to be suitable for the detection of significant prostate cancer as well. The structured reporting system for multiparametric MRI of the prostate according to PI-RADS Version 1 led to improved and reproducible diagnosis of prostate cancer. The new PI-RADS Version 2 aims to minimize the limitations of Version 1 and make PI-RADS standardization more globally acceptable.

Key Points:
- The detection, staging, and active monitoring of prostate cancer are common clinical questions.
- The best method for answering these questions is multiparametric MRI.
- Ultrasound elastography also seems to be suitable for the detection of significant prostate cancer.
- The new PI-RADS Version 2 claims to eliminate the limitations of PI-RADS Version 1 and to allow globally recognized standardized diagnostic reporting.

Citation Format:
- Franiel T, Asbach P, Teichgräber U et al. Bildgebung der Prostata – Ein Update. Fortschr Röntgenstr 2015; 187: 751–759

Zusammenfassung

Neue technische und klinische Entwicklungen auf dem Gebiet der Ultraschalldiagnostik und auf dem Gebiet der Magnetresonanztomografie haben die Detektion, Lokalisation und Staging sowie die aktive Überwachung des Prostatakarzinoms stark verbessert. Die beste Methode für diese typischen Fragestellungen ist die multiparametrische MRT. Die Ultraschallelastografie scheint ebenfalls für den Nachweis signifikanter Karzinome geeignet zu sein. Die strukturierte Befundung der multiparametrischen MRT der Prostata nach PI-RADS Version 1 führte zu einer verbesserten und nachvollziehbareren Diagnostik des Prostatakarzinoms. Die neue PI-RADS Version 2 versucht, die Limitationen der Version 1 zu minimieren und eine global akzeptierte Standardisierung zu erreichen.

Introduction

Prostate cancer is the most common cancer in Germany and the third most common cancer resulting in death in men [1]. Ultrasound and magnetic resonance imaging have developed very dynamically in recent years for the diagnosis of prostate cancer. These new technical and clinical developments are evaluated in the following after a short introduction regarding suitability for the detection, localization and staging and active monitoring of prostate cancer. Finally, the main differences and new developments of PI-RADS Version 2 compared to PI-RADS Version 1 introduced in 2012 are discussed.

Ultrasound

Transrectal ultrasound and color-coded Doppler ultrasound

The prostate is accessible with ultrasound. Transrectal ultrasound (TRUS) performed with endocavitary ultrasound probes provides very precise images of the prostate.

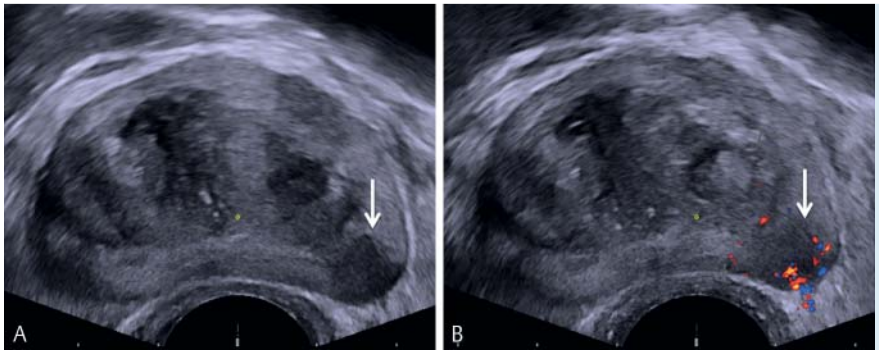

Fig. 1 TRUS image **A** with corresponding color-coded Doppler sonography **B** of the prostate of a 70-year-old patient with a PSA = 4.5 ng/ml (undergoing 5α reductase inhibitor treatment): A hypoechoic area suspicious for cancer in the left dorsolateral peripheral zone with sign of increased vascularization on color-coded Doppler sonography (arrow) is visible.

The strength of the received sound waves is coded in brightness mode (B-mode) as a grayscale image. The Doppler effect of moving reflective objects (blood) is utilized for color-coded Doppler sonography. The Doppler signals are registered by pulsed wave Doppler (PW Doppler) and the flow direction and rate are determined from the Doppler shift (discrepancy between frequency of echo and ultrasonic pulse). These are color-coded and superimposed on the B-mode image.

Prostate cancer is often hypoechoic on the B-mode image of TRUS (**Fig. 1A**) but can also be isoechoic or hyperechoic. This makes it difficult to detect and locate the prostate cancer. Although the specificity of 90 % is relatively high in this regard, the sensitivity is too low at 18 % [2]. For the detection of an extracapsular growth, the sensitivity is again low at 15 % (specificity 97 %) [2]. However, it could be shown that the positive predictive value regarding the presence of prostate cancer is elevated when signs of increased vascularization can be detected on color-coded Doppler sonography (**Fig. 1A**). Targeted specimen collection from these areas can be performed in these cases in addition to systematic biopsy in accordance with the S3 guideline (S3 guideline 2011). Due to the high level of uncertainty regarding undetected significant prostate cancers (Gleason score > 3 + 3, tumor volume ≥ 0.5 cm^3), this method is also not suitable for active monitoring in our opinion. Rather the prostate volume can be calculated with TRUS and the systematic extraction of core biopsies can be guided by imaging.

Ultrasound elastography

Elastography makes it possible to evaluate the elasticity and stiffness of tissue. In principle, there are two methods: conventional ultrasound strain elastography and ultrasound shear wave elastography. In the case of strain elastography, the tissue to be examined is compressed by the examiner using the ultrasound probe. The comparison of ultrasound images before and after compression makes it possible to make conclusions about the stiffness of the tissue based on the degree of deformation. Adequate application of compression and the interpretation of the color-coded images in real time are difficult to standardize and yield heterogeneous, examiner-dependent results. Another method is shear wave elastography in which the tissue is not compressed. Rather the shear waves are applied directly by the ultrasound probe and then disperse into the tissue (shear wave propagation). The stiffness of the tissue is calculated based on the propagation speed of the shear waves in the tissue. The main advantage of this method is the high intraindividual and interindividual reproducibility [3].

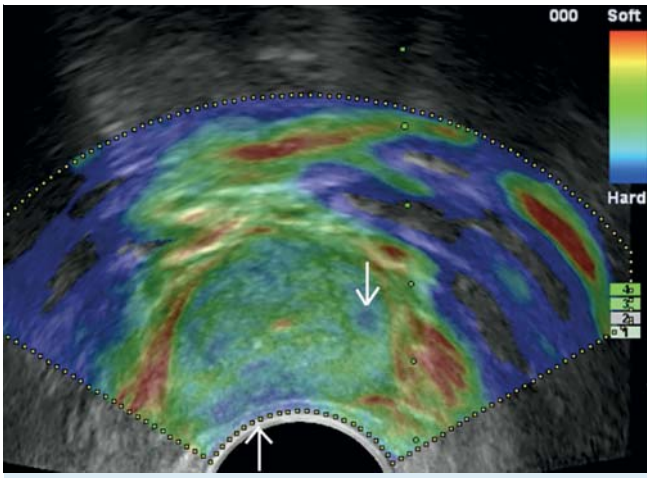

Fig. 2 TRUS image with strain elastography of a 70-year-old patient: Homogeneous prostate tissue of medium hardness (green) is visible. The region of the capsule or the neurovascular bundle and the urethra typically appear soft (red). Reproducible, clearly definable harder areas (blue) are visible as small foci left lateral in the region of the middle gland and right dorsal in the region of the middle gland (arrows). In the case of persistent PSA increase despite negative systematic 12-core biopsy, systematic saturation biopsy (24 cores) with additional targeted biopsy (4 cores) from areas suspicious on elastography is performed. 2 cores of the systematic biopsy (right lateral middle gland) and 2 cores of the targeted biopsy (left lateral middle gland) showed prostate cancer with a Gleason score 3 + 4.

In general, prostate cancer is characterized by increased stiffness compared to normal tissue (**Fig. 2**). However, areas with prostatitis, fibrosis, atrophy, or with benign prostate hyperplasia can also be associated with increased stiffness on ultrasound elastography. The resulting difficulty differentiating from prostate cancer leads to false-positive findings. False-negative elastography findings can be due to the architecture pattern of the particular prostate cancer [4]. In particular, prostate cancers with a Gleason score ≤ 7a often show a diffuse pattern with normal tissue and prostate cancer cells next to one another. However, if the prostate cancer is comprised of tumor cells that are close together, this results in stiff tissue and better detection on ultrasound elastography (**Fig. 3**) [5].

A study with 230 patients with a systematic 10-core biopsy combined with a targeted 5-core biopsy from areas suspicious on elastography was able to show that cancer could be detected with targeted biopsy in 30 % of cases while sys-

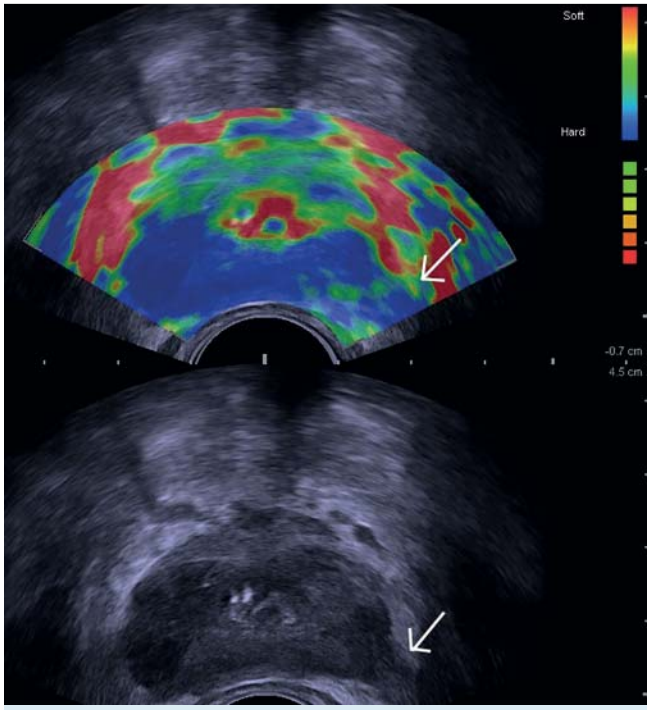

Fig. 3 Simultaneous TRUS image (bottom: ultrasound alone; top: ultrasound and superimposed strain elastography image) of the prostate of an 84-year-old patient with locally advanced prostate cancer (Gleason score 3 + 4): Areas with increased hypoechogenicity can be seen on ultrasound in the peripheral zone from right to left. The contour of the prostate is irregular or absent (in particular left lateral, arrow). The surface of the entire peripheral gland appears hard on elastography. A left peripheral growth exceeding the capsule (arrow) is very probable. The ventral periprostatic tissue and the region of the urethra appear soft.

tematic biopsy detected a cancer in only 25 % of cases. Due to major overlapping of the detected cancers of the two biopsy approaches, the combination of the two methods detected prostate cancer in 35 % of patients [6].. A newer study including 1024 patients with a systematic 10-core biopsy combined with a targeted 4-core biopsy from areas suspicious on elastography came to the conclusion that prostate cancer could be detected with targeted biopsy in 29 % of cases, with systematic biopsy in 39 % of cases, and with the combination of the two approaches in 46 % of cases [7]. Since it was also able to be shown with this study that the combination of both methods detects more cancers than targeted or systematic biopsy alone, ultrasound elastography should only be used for the detection of prostate cancer in combination with systematic biopsy. It was also interesting in this study that 34 patients with a significant prostate cancer could only be detected by ultrasound elastography [7]. A further study including 127 patents with a systematic 10-core biopsy combined with a targeted 4-core biopsy from areas suspicious on elastography was able to show that the targeted biopsy increased the negative predictive value from 79 % to 97 % for the presence of high-grade prostate cancer [8]. This means that negative elastography rules out high-grade prostate cancer with high probability. These results indicate that elastography has great potential to be helpful for select patients undergoing active monitoring. In regression analysis, it could also be shown that positive elastography is an independent marker for high-grade prostate cancer [8].

For determining the location of the prostate cancer with the help of ultrasound elastography, it was shown that the accuracy depends on the size and volume of the cancer [9]. Accordingly, the location of a prostate cancer with a diameter of 6 – 10 mm could be correctly determined in 27 % of cases, with a diameter of 11 – 20 mm in 71 % of cases and with a diameter of > 20 mm in 100 % of cases. The location of cancers with a volume of ≥ 0.5 cm³ was correctly determined in 91 % of cases [9]. A current study regarding ultrasound-guided shear wave elastography achieved a diagnostic accuracy of 74 % (sensitivity 81 %, specificity 69 %) in a validated cohort with a cut-off value of a stiffness of 50 kPa [10]. In contrast, the detection of an extracapsular growth was achieved with an only insufficient sensitivity of 38 % and a specificity of 96 % [2]. Due to the insufficient sensitivity for detecting an extracapsular growth, the method should not be routinely used for staging.

A study combining ultrasound elastography with multiparametric MRI was able to show that the combination of the two methods correctly determined the location of 92 % of all cancers [9]. In this study the sole use of multiparametric MRI would have correctly located the cancer in 87 % of cases and the sole use of elastography in 67 % of cases. However, this difference was only statistically significant for prostate cancer is a very anterior location or in the transitional zone ($p = 0.03$). However, these areas in particular are clinically relevant since approx. 41 % of prostate cancers were found in patients with at least one negative systematic biopsy and also an increased PSA value suspicious for cancer in the targeted MRI-based follow-up biopsy [11].

Contrast-enhanced ultrasound

For various issues, ultrasound can be enhanced by the use of ultrasound contrast agents. Ultrasound contrast agents are comprised of gas-filled microbubbles. The microbubbles begin to oscillate in the ultrasound field and these nonlinear oscillations can be effectively differentiated from the linear signals of the tissue. This then results in increased contrast of highly vascular prostate areas compared to minimally vascularized areas [12]. The main disadvantage of this method in our opinion is the relatively short examination time since in particular the wash-in phase of the contrast is greatest between highly vascularized prostate cancer and less vascularized normal prostate tissue. Since this phase is generally not longer than 10 seconds, the examination of the entire prostate is very difficult. In practice, usually only the areas that appear suspicious on B-mode images can be further clarified.

A prospective randomized clinical study compared the detection rate of the combination of systematic TRUS-guided biopsy and targeted biopsy of areas suspicious on contrast-enhanced ultrasound with the detection rate of systematic biopsy alone in patients with a serum PSA value between 2.5 – 9.9 ng/ml [13]. This study could not prove any statistically significant difference between the two approaches ($p = 0.33$). In detail, the detection rate of the combined approach was 31 % and that of systematic biopsy alone was 29 % [13]. A prospective randomized multicenter phase 3 study with the goal of proving a 6 % better detection rate by using contrast- enhanced ultrasound compared to systematic biopsy alone was ended early since the study goal

was no longer achievable at the time of study termination (http://clinicaltrial.gov/ct2/show/NCT00 911 027). These results suggest that contrast-enhanced ultrasound is not suitable for detection. We do not know of current data regarding localization, staging and active monitoring with the help of contrast-enhanced ultrasound. However, it is obvious that an insufficient detection accuracy is probably also associated with an insufficient localization accuracy and this entails high unreliability regarding undetected significant prostate cancers. Therefore, contrast-enhanced ultrasound should not be used for localization and staging and for selecting suitable patients for active monitoring according to current data.

Computer-assisted ultrasound

HistoScanning™ and computer-assisted TRUS based on an artificial neuronal network analysis (ANNA/C-TRUS) are two methods in which raw ultrasound data or B-mode images are post-processed so that conclusions about the presence of prostate cancer can be made.

The computer-based technology HistoScanning™ works with conventional TRUS. The raw TRUS data are processed by characterization algorithms developed specifically for this purpose and a three-dimensional image of the prostate is then generated. Suspicious areas are marked in color [14]. In the past very positive data for HistoScanning™ was published by one center. However, current publications provide different data. With regard to the detection of prostate cancer, it was able to be shown in a current study that systematic biopsy detected more prostate cancers compared to HistoScanning™. Prostate cancer was found in 63 % of the examined patients with systematic biopsy while this was the case in only 38 % of patients with HistoScanning™ [15]. The comparison of the detection rate of HistoScanning™ with the results of systematic perineal biopsy yielded comparable results. A prostate cancer could be detected in only 13 % of patients with HistoScanning™ in one study while systematic transperineal biopsy detected prostate cancer in 54 % of patients [15]. A further study with 198 evaluated patients used HistoScanning™ for prediction accuracy of a subsequent sextant biopsy. A diagnostic accuracy of HistoScanning™ for the detection of prostate cancer of 0.58 was seen here [16]. This insufficient detection accuracy is in agreement with a suboptimal localization accuracy of tumors ≥ 0.2 cm^3. Therefore, this method does not seem suitable for staging [15]. The cancer volume determined with HistoScanning™ did not coincide with the actual volume in the prostatectomy specimen [17]. A correlation analysis also showed no diagnostically usable correlation coefficient ($r_s = -0.0083$, $p = 0.9$). To our knowledge, no studies regarding the suitability of HistoScanning™ for active monitoring have been published yet. However, the insufficient detection accuracy and the lack of ability to determine tumor volume indicate that significant prostate cancers cannot be reliably ruled out with HistoScanning™.

ANNA/C-TRUS GmbH provides a neuronal and database-supported analysis system with parameters for detecting pathological areas in the prostate which was created on the basis of histopathologically verified comparisons between ultrasound images and the specimens of the radical prostatectomy in a series of 136 patients [18]. Using conventional TRUS, the examiner saves images of all representative transverse planes at intervals of 5 mm and transfers them to the server of ANNA/C-TRUS GmbH. The images are analyzed by ANNA/C-TRUS GmbH and the results are sent to the examiner.

There are only a few studies regarding the ANNA/C-TRUS technology. To date, it was able to be shown that prostate cancer was able to be detected in 31 of 75 patients (41 %) via targeted 6-core biopsy of areas suspicious on ANNA-C-TRUS [19]. These results were able to be confirmed in another study with 20 patients. Prostate cancer was able to be detected via biopsy of suspicious areas in 11 of 20 patients (58 %) [20]. A comparison of the results of targeted biopsy of suspicious areas and systematic biopsy has not yet been published. Due to the low number of studies published to date, a final evaluation of this method is currently not possible in our opinion.

Multiparametric Magnetic Resonance Imaging

Multiparametric MRI (mpMRI) is comprised of morphological T2-weighted imaging (T2w), diffusion-weighted imaging (DWI), dynamic contrast-enhanced MRI (DCE-MRI), and ^{1}H-magnetic resonance spectroscopy (^{1}H-MRS).

T2-weighted imaging provides the most important anatomical information in mpMRI. Prostate cancer has a low signal in T2 weighting. The quantification of the T2 signal intensity via dedicated mapping sequences was examined in initial studies of small cohorts with respect to feasibility [21]. There are currently no larger prospective studies for detecting and localizing prostate cancer with this method.

DWI measures Brownian molecular motion of water molecules. In MRI the motion of the hydrogen in water molecules can be represented by the signal loss between two refocusing pulses [22]. To eliminate the T2 shine-through effect, the apparent diffusion coefficient (ADC) is calculated from the signal intensities of 2 or more diffusion weights. In general due to the higher cell density and the increased intracellular and intercellular proteins, prostate cancer has increased diffusion restriction compared to normal prostate tissue [23]. For this reason, prostate cancer is typically characterized by a lower ADC value than normal tissue and correspondingly increased signal intensities on diffusion-weighted images.

DCE-MRI continuously measures the signal intensities in prostate tissue after administration of an intravenous bolus of a non-specific extracellular gadolinium-based contrast agent. In comparison to normal tissue, prostate cancer is characterized in general by an earlier start of the signal increase, a steeper increase of the signal intensity time curve, a higher absolute signal intensity level, and a more significant drop in signal intensities over the further time course [24]. These signal intensity time curves form the foundation for all modeling in pharmacokinetic models. The most common pharmacokinetic model is the open two-compartment model according to Tofts with the parameters transfer constant (K^{trans}), rate constant (k_{ep}), and extracellular extravascular space (EES) [25].

In contrast, ^{1}H-MRS allows noninvasive evaluation of the chemical composition of the prostate. The received frequency spectrum is disassembled via Fourier transformation into the individual frequencies which are shown in parts per million (ppm) of the resonance frequency of tri-

methylsilyl propionate on the abscissa with the corresponding signal intensity on the ordinate [26]. The important metabolites for prostate diagnosis are choline at 3.2 ppm, citrate at 2.6 ppm, and creatine at 3.0 ppm. For the evaluation of prostate tissue, the ratio of the concentrations of choline + creatine/citrate is calculated.

The main clinical application of mpMRI of the prostate in Germany is the detection of cancer. It could be shown for the detection of significant prostate cancers that the combination of T2 W + DWI + DCE-MRI achieves a diagnostic accuracy of 0.90 [27]. Adding ^{1}H-MRS did not result in an increase in the diagnostic accuracy. The diagnostic detection accuracy of all significant and not significant prostate cancers was 0.85 in this study [27]. Compared to conventional urological diagnosis (palpation finding, serum PSA value, and prostate volume), it was able to be shown that the diagnostic accuracy for the detection of significant prostate cancers increased from 0.81 to 0.91 with the use of MRI [28]. This result was independent of the field strength of the MRI unit (1.5 or 3.0 Tesla) [28]. MRI-guided biopsy of the prostate performed at specialized centers was used in the past for histology in areas suspicious on MRI [29]. It was able to be shown that this approach detected 89.4 % fewer low-risk prostate cancers and 17.7 % more intermediate/high-risk prostate cancers compared to diagnosis with systematic TRUS-guided biopsy. The negative predictive value for the detection of an intermediate or high-risk prostate cancer was 97 % for the MRI approach and 72 % for systematic TRUS-guided biopsy [30]. The argument that the MRI strategy is more expensive than the TRUS strategy can be refuted. It was able to be shown that both strategies incur approximately the same costs [31]. In addition, the MRI strategy results in a reduction of the overdiagnosis and overtreatment of low-risk prostate cancers and thus in improved quality of life compared to the TRUS strategy [31].

An alternative to targeted MRI-guided biopsy is targeted TRUS-guided biopsy after cognitive fusion with the MRI images or targeted TRUS-guided biopsy after previous fusion with the MRI images (▶ **Fig. 4, 5**). In principle, the last-mentioned method includes two technical approaches. The approach offered by most providers is the rigid fusion of MRI and ultrasound images. However, this type of fusion cannot anticipate any deformation of the prostate caused by the ultrasound probe. In contrast, newer systems provide elastic fusion and minimize this problem. The largest study on fusion biopsy published to date prospectively examined 1003 patients [32]. This study was able to show that targeted biopsy detected 30 % more high-risk prostate cancers (173 vs. 122 patients) and 17 % fewer low-risk prostate cancers (213 vs. 258 patients) with fewer core biopsies than systematic TRUS-guided biopsy. By adding systematic biopsy to targeted biopsy, prostate cancer could additionally be verified in 103 patients but the cancer was a low-risk prostate cancer in 86 cases (83 %) and a high-risk prostate cancer in only 5 cases (5 %) [32]. Moreover, it was shown that for every high-risk prostate cancer additionally found with systematic biopsy 200 patients had to undergo both systematic and targeted biopsy [32].

Exact localization is required for proper staging. Like detection, a combination of T2w, DWI, and DCE-MRI makes sense for localization. The corresponding diagnostic accuracies are between 0.76 and 084 [33, 34]. In contrast, high-resolution T2w TSE sequence is the decisive sequence for the detection of extracapsular growth. In a metaanalysis from 2001, a diagnostic accuracy of 74 % could be shown for the detection of an extracapsular growth [35]. Current data from 2013 prove that the diagnostic accuracy for the detection of an extracapsular growth stays almost constant at 0.73 even using new 3-Tesla units and an endorectal coil [44]. This constantly good diagnostic accuracy is the reason why MRI verifiably increases the surgical decision for or against preservation of the neurovascular bundle in patients prior to planned radical prostatectomy [36].

In contrast to Germany, MRI of the prostate is performed as part of active monitoring in Great Britain according to the National Institute for Health and Care Excellence (NICE) guideline for prostate cancer in all patients in whom active monitoring is planned or in whom unclear PSA and clinical changes occur during active monitoring [37]. The reason for this is that prostate cancer cannot always be characterized with sufficient accuracy by systematic TRUS-guided biopsy. This is true in particular for anterior and apical prostate cancers [38]. Prostate cancers with a volume of > 0.5 cm³ are detected with the help of MRI with a diagnostic accuracy of 0.91 to 0.94 [39]. If the Gleason score is taken into consideration in this analysis, the sensitivity for the detection

Fig. 4 Multiparametric MRI at 1.5 T using an endorectal coil in the patient from Fig. 1: The T2w image **A** shows a hypointense area suspicious for cancer in the left dorsolateral peripheral zone without protrusion or infiltration of the capsule. The pharmacokinetic parameter map **B** calculated with the signal intensities (SI) of DCE-MRI has focally increased values suspicious for cancer left dorsolateral compared to the surrounding tissue. The SI-t curve is type III (not shown). Focally decreased diffusion coefficient values suspicious for carcinoma (coded blue) with correspondingly elevated SI on the b = 800 image (not shown) are located at the same location on the ADC map **C**. The corresponding cumulative score of the PI-RADS classification in version 1 is 4 + 5 + 5 = 14; this corresponds to a PI-RADS score V. According to version 2 of the PI-RADS classification, the area on DWI corresponds to a PI-RADS score IV since it is smaller than < 1.5 cm. The scoring of the T2w image and DCE-MRI is not important here.

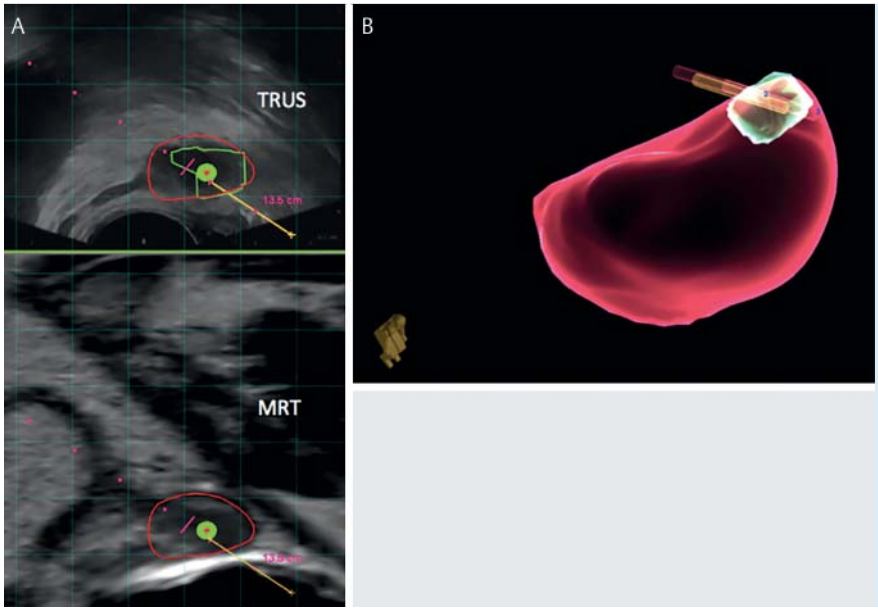

Fig. 5 After elastic fusion of the MRI images with the TRUS images (**A**), the prostate has a red border. The area suspicious for cancer marked on the T2w image (see Fig. 5) has a green border on the TRUS image. The TRUS-guided biopsy direction is shown as a red dotted line. The biopsy is taken when the "target" (green circle with red point) is in the suspicious area. (**B**) shows the prostate registered in TRUS with the suspicious area and the position of the 3 targeted TRUS-guided core biopsies. Prostate cancer with a Gleason score 4 + 4 (70 – 80 % of the biopsy surface) was detected in all 3 biopsies. Systematic TRUS-guided biopsy could not detect any further areas of prostate cancer.

of prostate cancer with a Gleason score of 3 + 3 is less than 0.65 for small cancers but increases to values of greater than 0.9 as the tumor volume increases. For prostate cancers with a Gleason score > 6, the sensitivity for the detection of prostate cancer was greater than 0.8 already for small volumes and increases to almost 100 % as the volume increases [39]. In simple terms this could mean in practice that a negative MRI (no unclear, probably or highly probably malignant areas) is a major indication of the suitability of the patient for active monitoring. In a current prospective study with 150 patients and a systematic transperineal 30-core biopsy as the gold standard it was able to be shown that a PI-RADS score of 1 or 2 (highly probably or probably benign areas) was associated with a moderate-risk prostate cancer only with a probability of 1.3 % [35]. A high-risk prostate cancer was not found in any patient with a PI-RADS score of 1 or 2 in this study [28].

MR elastography

The basic physical principle of elastography is the controlled shifting of tissue layers with shear waves. The propagation speed of shear waves depends on the shear modulus which is a measure of stiffness. The shear modulus can be measured via medical imaging by direct visualization of shear waves (mechanical imaging) [40]. MR elastography (MRE) is based on time-resolved imaging using shear waves propagating through the body. These shear waves are generated by a unit (actuator) needed in addition to the MRI unit and are coupled into the body surface of the patient. The shear waves are then recorded via motion-sensitive MRI sequences (phase contrast technique). Special inversion techniques can be used to generate a map of the organ stiffness (elastogram) from this time-resolved image dataset showing the stiffness in kilopascal (kPa). MR elastography for grading liver fibrosis is currently evaluated in multiple prospective studies and has been clinically established for a few years [41]. The necessary technology is now commercially available from different manufacturers. The potential advantage of MRE compared to ultrasound elastography is the possibility to acquire larger target volumes and a 3 D wave field which potentially results in a higher diagnostic accuracy. Only initial feasibility studies in healthy subjects and a few patients regarding MRE of the prostate are available (**Fig. 6**) [42]. An evaluation of the suitability for the detection and localization of prostate cancer is currently not possible.

PI-RADS classification version 1 and version 2

The introduction of PI-RADS classification in the first version (PI-RADS V1) 2 years ago resulted in increased acceptance of MRI of the prostate among urologists. In version 1a point value of 1 to 5 is assigned for every lesion and every multiparametric method [43]. A total score is then specified for every lesion that indicates the probability for a clinically significant prostate cancer with 1 being highly probably benign and 5 being high probably malignant [43]. To make this procedure objective, it was proposed to form a cumulative score from the individual scores [44]. The cumulative score can then be converted into the PI-RADS total score. This is independent of the number of methods used, ranges from 1 – 5 and can be easily communicated [27, 45]. Compared to diagnostic reporting without PI-RADS V1, the use of PI-RADS scores results in improved detection accuracy of 0.83 – 0.85 and increased interreader agreement [27, 46, 47]. The agreement between individual findings is good for prostate cancers (kappa values between 0.63 and 0.8) [46, 47].

The PI-RADS Version 2 classification (PI-RADS V2) introduced in December 2014 can be accessed since the start of 2015 as a PDF document under the link http://www.acr.org/Quality-Safety/Resources/PIRADS/ [48]. This version created together with the European Society of Urogenital Radiology (ESUR) and the American College of Radiology (ACR) claims to minimize the limitations of version 1 and to achieve globally accepted standardization. In contrast to PI-RADS V1, there are not yet any evaluation results for PI-

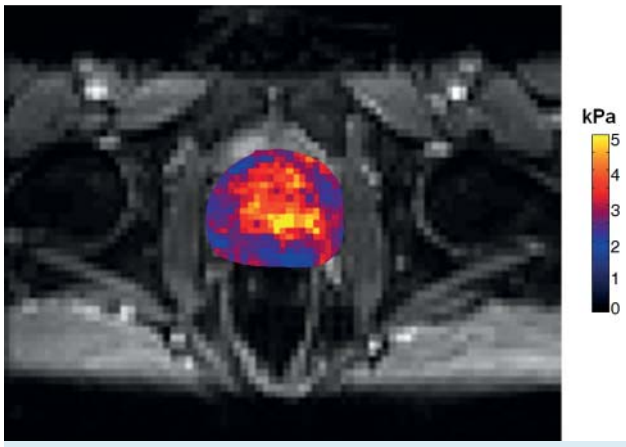

Fig. 6 MR elastography at 3 Tesla via EPI sequence using a body surface coil in a healthy 40-year-old patient. Perineal mechanical stimulation with frequencies of 60 Hz, 65 Hz, 70 Hz, 75 Hz and 80 Hz (acquisition time 3 minutes). The figure shows the elastogram calculated from the raw data via inversion. The stiffness of the prostate is color-coded and spatially resolved here (pixel size 3 × 3 mm) and is about 4 kPa.

RADS V2. Like version 1, the images of multiparametric MRI are exclusively used for classification. The classification as PI-RADS 1 – 5 is retained in version 2. However, ^{1}H-MRS is no longer taken into consideration for the PI-RADS evaluation. The formation of a cumulative score is also eliminated. Diffusion-weighted images are decisive for the evaluation of the peripheral zone and T2w images for the evaluation of the central gland regions (**Fig. 7**, **Table 1**). DCE-MRI plays only a subordinate role. It is needed for the further classification of PI-RADS 3 lesions (DWI) of the peripheral zone. Early focal enhancement of the suspicious lesion results in upgrading to category 4. The main difference between a finding with a score of 4 and a score of 5 in T2w and DWI is a diameter < 1.5 cm and ≥ 1.5 cm, respectively. No more than 4 lesions with a PIRADS score of 3 – 5 should be noted in the finding. For the case that more than 4 such lesions are present, the 4 lesions with the highest PI-RADS score are specified. At least the maximum size should be specified for each of these lesions. A further change relates to the sector model which now includes 39 regions: 36 for the prostate, 2 for the seminal vesicle, and 1 for the external sphincter of the urethra. For these regions easy-to-understand anatomy-based abbreviations are used instead of numbers.

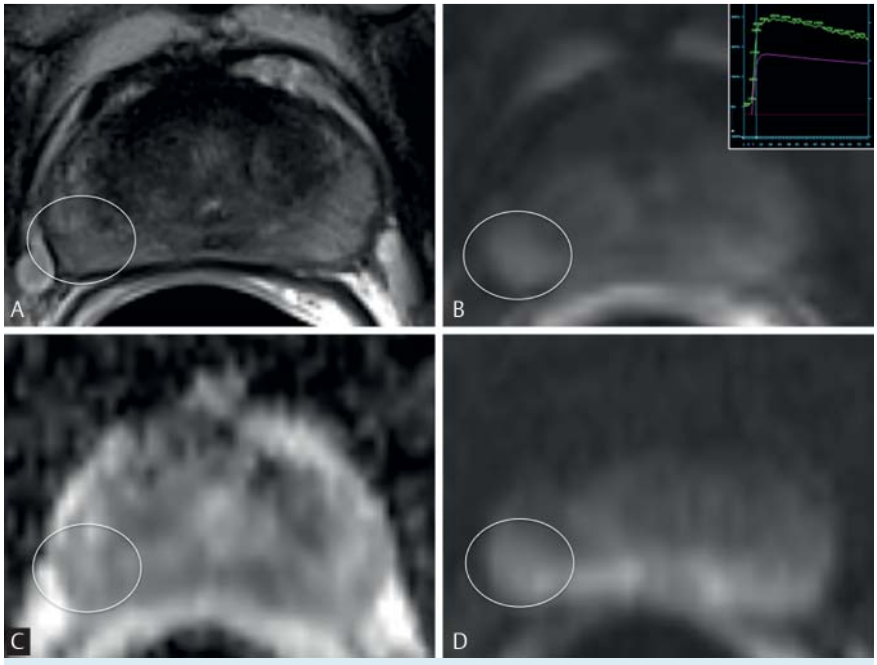

Fig. 7 Multiparametric MRI of the prostate of a 46-year-old patient with a PSA = 5.1 ng/ml. The T2w image **A** shows band-shaped, streaky, dull hypointensity in the peripheral zone of the middle gland right posterolateral (white circle). On DCE-MRI **B**, this area shows focal and early enhancement compared to the surrounding tissue. The corresponding SI-t curve (upper right in **B**) decreases in the further course after the maximum is reached. On the ADC map **C**, this area shows diffuse diffusion restriction with corresponding diffuse hyperintensity on the b-800 image of the DWI **D**. According to the PI-RADS V1 classification, 2 points were assigned for T2w, 2 points for DWI, and 4 points for DCE-MRI (focal and type III curve). This lesion was then evaluated with a total score of 3 (unclear finding). According to the PI-RADS V2 classification, T2w was evaluated with 2 points, DWI with 2 points, and DCE-MRI with "+" (early, focal enhancement). Since the lesion is in the peripheral zone, the point value of DWI is significant for the total score which is why the lesion was evaluated with a total score of 2 (probably benign finding). The score for T2w and the enhancement are not taken into account in this case for the total score according to PI-RADS V2 (**Table 1**). Normal prostate tissue with minimal inflammatory infiltrates was detected with core biopsy of the in-bore MRI-guided biopsy.

Summary

The common clinical issues involving the prostate include the detection, localization, staging, and active monitoring of prostate cancer. The most exact method for the detection of prostate cancer is multiparametric MRI. For the performance and interpretation of multiparametric MRI, the new PI-RADS Version 2 claims to eliminate the limitations of PI-RADS Version 1 and to allow globally recognized standardized diagnostic reporting. Areas classified as unclear, probably malignant, or highly probably malignant can either undergo targeted MRI-guided biopsy or targeted TRUS-guided biopsy after prior fusion with the MRI images. Significant prostate cancers are detected with both methods with high diagnostic accuracy. The latest studies regarding ultrasound elastography can prove that this method also seems suitable for detecting significant prostate cancers. In the future a biopsy could be extracted in a targeted manner during fusion biopsy from areas suspicious on MRI as well as from areas suspicious on ultrasound elastography. Alternatively, to confirm the results of elastography, MR elastography could be performed in addition to mpMRI and could be relatively easily integrated into the MRI protocol. The best imaging method for the localization

Table 1 PI-RADS V2 scoring system for the peripheral zone.

DWI	T2w	DCE-MRI	PI-RADS
1	all[1]	all	1
2	all	all	2
3	all	–[2]	3
		+[3]	4
4	all	all	4
5	all	all	5

[1] "all" stands for score 1 – 5
[2] "-" means no early enhancement or diffuse enhancement which does not correlate with the suspicious finding, or focal enhancement corresponding to typical BPH nodules
[3] "+" means early focal enhancement in the suspicious lesion

Table 2 PI-RADS V2 scoring system for the central gland.

T2w	DWI	DCE-MRI	PI-RADS
1	all[1]	all	1
2	all	all	2
3	1 – 4	all	3
	5	all	4
4	all	all	4
5	all	all	5

[1] "all" stands for score 1 – 5

and staging of prostate cancer is multiparametric MRI. The achieved diagnostic accuracies are between 0.73 and 0.84 depending on the study. The best imaging method for the selection of suitable patients for active monitoring is also multiparametric MRI. This can be used to detect intermediate/high-risk prostate carcinomas and carcinomas with a volume of > 0.5 cm^3 with high diagnostic accuracy. However, ultrasound elastography also seems helpful for the selection of suitable patients in this regard.

References

1 *Baras N, Barnes B, Bertz J et al.* Übersicht zu den Krebssterbefällen. In: Krebs in Deutschland. Robert Koch Institut(Hrsg). Berlin: 2013; 17
2 *Brock M, von Bodman C, Sommerer F et al.* Comparison of real-time elastography with grey-scale ultrasonography for detection of organ-confined prostate cancer and extra capsular extension: a prospective analysis using whole mount sections after radical prostatectomy. BJU international 2011; 108: E217 – E222
3 *Wells PN, Liang HD.* Medical ultrasound: imaging of soft tissue strain and elasticity. Journal of the Royal Society, Interface/the Royal Society 2011; 8: 1521 – 1549
4 *Langer DL, van der Kwast TH, Evans AJ et al.* Intermixed normal tissue within prostate cancer: effect on MR imaging measurements of apparent diffusion coefficient and T2–sparse versus dense cancers. Radiology 2008; 249: 900 – 908
5 *Junker D, Schafer G, Aigner F et al.* Potentials and limitations of real-time elastography for prostate cancer detection: a whole-mount step section analysis. TheScientificWorldJournal 2012; 2012: 193213
6 *Pallwein L, Mitterberger M, Struve P et al.* Comparison of sonoelastography guided biopsy with systematic biopsy: impact on prostate cancer detection. European radiology 2007; 17: 2278 – 2285
7 *Salomon G, Drews N, Autier P et al.* Incremental detection rate of prostate cancer by real-time elastography targeted biopsies in combination with a conventional 10-core biopsy in 1024 consecutive patients. BJU international 2014; 113: 548 – 553
8 *Nygard Y, Haukaas SA, Halvorsen OJ et al.* A positive real-time elastography is an independent marker for detection of high-risk prostate cancers in the primary biopsy setting. BJU international 2014; 113: E90 – E97
9 *Junker D, Schafer G, Kobel C et al.* Comparison of real-time elastography and multiparametric MRI for prostate cancer detection: a whole-mount step-section analysis. American journal of roentgenology 2014; 202: W263 – W269
10 *Boehm K, Salomon G, Beyer B et al.* Shear Wave Elastography for Localization of Prostate Cancer Lesions and Assessment of Elasticity Thresholds: Implications for Targeted Biopsies and Active Surveillance Protocols. J Urol 2015; 193: 794
11 *Schimmoller L, Quentin M, Arsov C et al.* Predictive power of the ESUR scoring system for prostate cancer diagnosis verified with targeted MR-guided in-bore biopsy. Eur J Radiol 2014; 83: 2103 – 2108
12 *Albrecht T, Blomley M, Bolondi L et al.* Guidelines for the use of contrast agents in ultrasound. January 2004. Ultraschall in der Medizin 2004; 25: 249 – 256
13 *Taverna G, Morandi G, Seveso M et al.* Colour Doppler and microbubble contrast agent ultrasonography do not improve cancer detection rate in transrectal systematic prostate biopsy sampling. BJU international 2011; 108: 1723 – 1727
14 *Braeckman J, Autier P, Garbar C et al.* Computer-aided ultrasonography (HistoScanning): a novel technology for locating and characterizing prostate cancer. BJU international 2008; 101: 293 – 298
15 *Javed S, Chadwick E, Edwards AA et al.* Does prostate HistoScanning play a role in detecting prostate cancer in routine clinical practice? Results from three independent studies. BJU international 2014; 114: 541 – 548
16 *Schiffmann J, Tennstedt P, Fischer J et al.* Does HistoScanning predict positive results in prostate biopsy? A retrospective analysis of 1188 sextants of the prostate. World journal of urology 2014; 32: 925 – 930
17 *Schiffmann J, Fischer J, Tennstedt P et al.* Comparison of prostate cancer volume measured by HistoScanning and final histopathological results. World journal of urology 2014; 32: 939 – 944
18 *Loch T.* Computerized supported transrectal ultrasound (C-TRUS) in the diagnosis of prostate cancer. Der Urologe Ausg A 2004; 43: 1377 – 1384
19 *Grabski B, Baeurle L, Loch A et al.* Computerized transrectal ultrasound of the prostate in a multicenter setup (C-TRUS-MS): detection of cancer after multiple negative systematic random and in primary biopsies. World journal of urology 2011; 29: 573 – 579
20 *Strunk T, Decker G, Willinek W et al.* Combination of C-TRUS with multiparametric MRI: potential for improving detection of prostate cancer. World journal of urology 2014; 32: 335 – 339
21 *Liu W, Turkbey B, Senegas J et al.* Accelerated T2 mapping for characterization of prostate cancer. Magnetic resonance in medicine: official journal of the Society of Magnetic Resonance in Medicine/Society of Magnetic Resonance in Medicine 2011; 65: 1400 – 1406
22 *Stejskal EO, Tanner JE.* Spin diffusion measurements: spin echos in the presence of a time dependent field gradient. J Chem Phys 1965; 42: 288 – 292
23 *Langer DL, van der Kwast TH, Evans AJ et al.* Prostate tissue composition and MR measurements: investigating the relationships between ADC, T2, K(trans), v(e), and corresponding histologic features. Radiology 2010; 255: 485 – 494
24 *Franiel T, Hamm B, Hricak H.* Dynamic contrast-enhanced magnetic resonance imaging and pharmacokinetic models in prostate cancer. Eur Radiol 2011; 21: 616 – 626
25 *Tofts PS, Brix G, Buckley DL et al.* Estimating kinetic parameters from dynamic contrast-enhanced T(1)-weighted MRI of a diffusable tracer: standardized quantities and symbols. J Magn Reson Imaging 1999; 10: 223 – 232
26 *Franiel T.* Multiparametrische Magnetresonanztomografie der Prostata – Technik und klinische Anwendungen. Fortschr Röntgenstr 2011; 183: 607 – 617
27 *Roethke MC, Kuru TH, Schultze S et al.* Evaluation of the ESUR PI-RADS scoring system for multiparametric MRI of the prostate with targeted MR/TRUS fusion-guided biopsy at 3.0 Tesla. Eur Radiol 2014; 24: 344 – 352
28 *Thompson JE, Moses D, Shnier R et al.* Multiparametric Magnetic Resonance Imaging Guided Diagnostic Biopsy Detects Significant Prostate Cancer and could Reduce Unnecessary Biopsies and Over Detection: A Prospective Study. J Urol 2014; 192: 67 – 74
29 *Franiel T, Stephan C, Erbersdobler A et al.* Areas suspicious for prostate cancer: MR-guided biopsy in patients with at least one transrectal US-guided biopsy with a negative finding – multiparametric MR imaging for detection and biopsy planning. Radiology 2011; 259: 162 – 172

30 *Pokorny MR*, *de Rooij M*, *Duncan E et al.* Prospective study of diagnostic accuracy comparing prostate cancer detection by transrectal ultrasound-guided biopsy versus magnetic resonance (MR) imaging with subsequent MR-guided biopsy in men without previous prostate biopsies. Eur Urol 2014; 66: 22 – 29
31 *de Rooij M*, *Crienen S*, *Witjes JA et al.* Cost-effectiveness of magnetic resonance (MR) imaging and MR-guided targeted biopsy versus systematic transrectal ultrasound-guided biopsy in diagnosing prostate cancer: a modelling study from a health care perspective. Eur Urol 2014; 66: 430 – 436
32 *Siddiqui MM*, *Rais-Bahrami S*, *Turkbey B et al.* Comparison of MR/ultrasound fusion-guided biopsy with ultrasound-guided biopsy for the diagnosis of prostate cancer. JAMA 2015; 313: 390 – 397
33 *Vargas HA*, *Akin O*, *Franiel T et al.* Diffusion-weighted endorectal MR imaging at 3 T for prostate cancer: tumor detection and assessment of aggressiveness. Radiology 2011; 259: 775 – 784
34 *Beyersdorff D*, *Lüdemann L*, *Dietz E et al.* Dynamische kontrastmittelgestützte MRT der Prostata: Vergleich von zwei Auswerteverfahren. Fortschr Röntgenstr 2011; 183: 456 – 461
35 *Sonnad SS*, *Langlotz CP*, *Schwartz JS*. Accuracy of MR imaging for staging prostate cancer: a meta-analysis to examine the effect of technologic change. Acad Radiol 2001; 8: 149 – 157
36 *Hricak H*, *Wang L*, *Wei DC et al.* The role of preoperative endorectal magnetic resonance imaging in the decision regarding whether to preserve or resect neurovascular bundles during radical retropubic prostatectomy. Cancer 2004; 100: 2655 – 2663
37 *Graham J*, *Kirkbride P*, *Cann K et al.* Prostate cancer: summary of updated NICE guidance. Bmj 2014; 348: f7524
38 *Hambrock T*, *Somford DM*, *Hoeks C et al.* Magnetic resonance imaging guided prostate biopsy in men with repeat negative biopsies and increased prostate specific antigen. J Urol 2010; 183: 520 – 527
39 *Vargas HA*, *Akin O*, *Shukla-Dave A et al.* Performance characteristics of MR imaging in the evaluation of clinically low-risk prostate cancer: a prospective study. Radiology 2012; 265: 478 – 487
40 *Sack I*, *Fischer T*, *Thomas A et al.* Magnetic resonance elastography of the liver. Der Radiologe 2012; 52: 738 – 744
41 *Singh S*, *Venkatesh SK*, *Wang Z et al.* Diagnostic Performance of Magnetic Resonance Elastography in Staging Liver Fibrosis: A Systematic Review and Meta-analysis of Individual Participant Data. Clin Gastroenterol Hepatol 2015; 13: 440 – 451
42 *Sahebjavaher RS*, *Nir G*, *Honarvar M et al.* MR elastography of prostate cancer: quantitative comparison with histopathology and repeatability of methods. NMR in biomedicine 2015; 28: 124 – 139
43 *Barentsz JO*, *Richenberg J*, *Clements R et al.* ESUR prostate MR guidelines 2012. Eur Radiol 2012; 22: 746 – 757
44 *Röthke M*, *Blondin D*, *Schlemmer HP et al.* PI-RADS-Klassifikation: Strukturiertes Befundungsschema für die MRT der Prostata. Fortschr Röntgenstr 2013; 185: 253 – 261
45 *Schimmoller L*, *Quentin M*, *Arsov C et al.* MR-sequences for prostate cancer diagnostics: validation based on the PI-RADS scoring system and targeted MR-guided in-bore biopsy. Eur Radiol 2014; 24: 2582 – 2589
46 *Renard-Penna R*, *Mozer P*, *Cornud F et al.* Prostate Imaging Reporting and Data System and Likert Scoring System: Multiparametric MR Imaging Validation Study to Screen Patients for Initial Biopsy. Radiology 2015; 275: 458 – 468
47 *Schimmoller L*, *Quentin M*, *Arsov C et al.* Inter-reader agreement of the ESUR score for prostate MRI using in-bore MRI-guided biopsies as the reference standard. Eur Radiol 2013; 23: 3185 – 3190
48 American College of Radiology. MR Prostate Imaging Reporting and Data System version 2.0. from http://www.acr.org/Quality-Safety/Resources/PIRADS/